

PROTON BEAM ACCELERATION UP TO 160 MeV
AT THE MOSCOW MESON FACTORY LINAC

G.I.Batskich*, Yu.V.Bylinsky, S.K.Esin, A.P.Fedotov,
A.V.Feschchenko, Yu.D.Ivanov*, O.S.Korolev, L.V.Kravchuk,
A.I.Kvasha*, V.A.Matveev, V.N.Michailov*, A.N.Mirzozjan,
N.P.Murin*, P.N.Ostroumov, S.A.Petronevich, B.A.Rubtsov*,
V.L.Serov, S.I.Scharamentov, N.I.Uksusov*, S.Zy.Zyarylkapov
I.A.Sagin

Institute for Nuclear Research of the Academy of Sciences of the
USSR, Moscow, 117312, USSR

* Moscow Radiotechnical Institute, Moscow, 113519, USSR

Abstract

The H^+ , H^- linac of the INR meson factory designed for accelerating of the 0.5 mA average current beam to the energy up to 600 MeV is under tuning in Troitsk near Moscow. The results of the tuning of the drift tube linac operating at the frequency of 198.2 MHz with the output proton energy of 100 MeV, followed by the four disk and washer (DAW) cavities operating at the frequency of 991 MHz with the output energy of 160 MeV, are presented.

The layout and features of 160 MeV
part of the linac

Recently the tuning experience of the first Alvarez tank with the output energy of 20.45 MeV was presented in ref [1].

The first stage of the linac with the output energy of 100 MeV consists of the five tanks with drift tubes operating at the frequency of 198.2MHz. The first stage is followed by the four resonant cavities with disks and washers operating at the frequency of 991 MHz, where protons are accelerated to the energy of 160 MeV.

The first four tanks of the first stage are long. For example the first of them is 3.8 longitudinal oscillation wave length long. The fifth one is a quarter wavelength long. Besides accelerating (from 94 MeV to 100 MeV the fifth tank is designed to reduce the phase length of bunches by 1.4 times (increasing respectively the momentum spread) so that the bunches should fit safely in the longitudinal acceptance of the second stage of the linac [2].

Transition from the first to the second stages of the linac is the main feature to be taken into account when tuning the accelerator.

The layout of the first and of the opening part of the second stages of the linac together with the measuring equipment is shown in fig. 1 and fig. 2. After tuning of the first stage of the linac the measuring equipment, installed at its output, was moved to the 160 MeV output.

In the course of tuning the injector was driven at 1 Hz repetition rate to avoid the excessive activation of the equipment. Tanks and resonant cavities were driven at 10 Hz.

The first 100 MeV stage of the linac.

The rf amplitude and phase setting in resonant cavities plays the major role in tuning process. For rf phase setting in a resonant cavity the dependence of the accelerated current on the rf phase difference between the tuned and the preceding resonant cavities $I(\varphi)$ was used. The dependence was calculated and measured experimentally. The selection of the accelerated particles was mode with the aid of the absorbing foil which let pass through it only the particles, accelerated in the resonant cavity under tuning. Absorbing foils were placed at the output of the fifth tank.

The calculated dependencies $I(\varphi)$ for the second tank for different by 5% within the range from 0.9 up to 1.1 of the nominal amplitude are shown in fig. 3. They may be used to ascertain the bucket width at a half-height level (ΔF). The nominal rf amplitude is determined by the nominal bucket width. The synchronous phase is found by the nominal rf amplitude of the calculated displacement from the front curve of phase scanning.

The aforementioned method requires the beam cutoff and may be used only for tuning at the small average beam current. Therefore the method for rf phase and amplitude setting based on the dependence of a certain harmonic of a beam current measured by the cavity monitor at the output of the accelerating cavity under tuning on the rf phase difference between this cavity and the preceding one, was proposed and used. A beam current harmonic is maximal if the bunches fit in the bucket; if the bunches exceed the bucket it is reduced due to debunching. The calculated dependence of the field level induced in the third-harmonic cavity monitor on the rf phase in the second tank is shown in fig. 4.

The accelerated beam current beyond the foil and its third harmonic were measured. The calculated and measured rf bucket width at the half-height level in the second tank got with the aid of the method based on the beam bunch harmonic monitor BHM is shown in fig.5. The rf amplitude and phase setting accuracy in the third and the fourth tanks with the aid of absorbing foils is 1% and 2% respectively. The method based on measuring of the third harmonic of the current is a bit less accurate.

The aforementioned rf amplitude and phase setting method is out suitable for the fifth short tank, in which the beam energy is just

slightly increased and bunches remain compact for a wide range of phase changes and slopes of the curve $I(\varphi)$ are eroded. Therefore for rf amplitude and phase setting in the fifth tank another methods were proposed, which are based on the dependence of the transit time of particles $\Delta\Phi$ in the tank on the rf phase in it.

The layout of transit time measurement is shown in fig. 6. Results of the calculation of functions $\Delta\Phi(\varphi)$ for which $\Delta\Phi$ value corresponds to the base (BHM2 - BHM3) are shown in fig. 7. Rf amplitude ranging from zero to 1.2 of the nominal level with the step 0.2 is the parameter of the curves.

Calculated and experimental maximum phase swing of the signal, induced in BHMs between extremums as functions of the rf amplitude in the fifth tank which enable one to determine nominal rf amplitude is shown in fig. 8.

The investigation of the focusing conditions was complicated by getting out of order quadrupole lenses in the fourth and the ninth drift tube of first tank. To solve the problem gradients of the opening eight drift tubes were retuned so that the transverse phase portrait of the beam should be nominal in the center of the tenth quadrupole lens. As a result the beam in the first stage of the linac was accelerated practically without losses. The maximum accelerated current was 23 mA. The characteristic transverse profile of the beam at the output of the fifth tank is shown in fig. 9.

The 100-160 MeV stage of the linac

First of all the nominal proton beam energy (100.1 \pm 0.2 MeV) at the output of the first stage of the linac was accurately set by fixing the rf amplitude in the fifth tank which was roughly calculated with the bending magnet at the 160 MeV output of the linac calibrated to the energy of 94.41 MeV at the output of the fourth tank. The momentum spectrum of the particles at the output of the first linac stage is shown in fig. 10. The spectrum width at the half-height level is 0.6%. The phase spectrum of the beam bunches at the output of the first stage of the linac measured with the aid of a bunch shape monitor [3] is shown in fig. 11.

Rf amplitudes and phases in the resonant cavities NN 6-9 of the second stage of the linac were set according to the following procedure. The rf amplitude in all the cavities was determined by the power introduced in a cavity and by its shunt impedance. The rf phase setting was based on the two simultaneously measured functions: the beam current harmonic at the output of a cavity under tuning and the beam current downstream the bending magnet, both depending on the scanned rf phase in that cavity. These functions for the seventh resonant cavity are shown in fig. 12.

Summary

1. The first stage of the linac (output energy 100.1 MeV, impulse current without buncher - 23 mA) and the opening part of the second stage with the output energy 158.6 MeV (impulse current without buncher - 10 mA) have been tuned.

2. Besides traditional methods and appliances for tuning were proposed and tested new ones: rf amplitude and phase setting by phase scanning with the aid of 1) the beam current harmonic monitor together with magnetic spectrum analyzer and 2) with the aid of bunch shape monitor.

3. At the 100 \div 160 MeV part of the linac DAW cavities were tested successfully. The influence of parasite modes on the beam was not registered.

4. The longitudinal parameters of the beam at the output of the first stage of the linac (phase length of bunches of 13 degrees measured with the bunch length monitor and momentum spread of \pm 0.76% measured with magnetic analyzer) are a bit better than designed. Therefore the beam losses due to longitudinal motion in the downstream part of the linac at the designed current of 50 mA are likely to be negligible.

Acknowledgment

Coauthors express their deep gratitude to scientists, engineers and technicians of many organizations taking part in MMF linac construction.

References

1. Ju.V.Bylinsky et al. Particle Accelerators, v.27, 1990, p. 107-112.
2. Ion Linear Accelerators, ed. by B.P.Murin, v.1,2. Moscow, 1978 (in russian).
3. A.V.Feschenko, P.N.Ostroumov. Proceedings of the 1986 Linac Conf., Stanford, June 2-6, 1986, p.323.

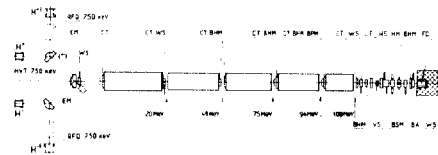


Fig. 1. The layout of the first stage of the linac with the measuring equipment.

Legend:
EM - emittance monitor, WS - wire scanner, CT - current monitor, BHM - bunch harmonic monitor, BPM - beam position monitor, HS, VS - horizontal and vertical slits, HM - halo monitor, FC - Faraday cup, BSM - bunch shape monitor, BA - beam absorbers

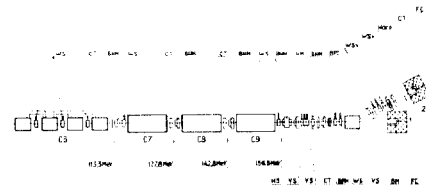


Fig. 2. The layout of the 100-160 MeV part of the linac

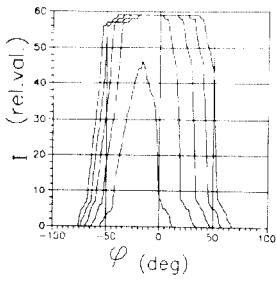


Fig. 3. The beam current beyond the absorber with the cutoff energy of 43 MeV as functions of rf phase in the second tank

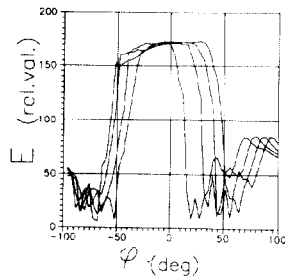


Fig. 4. The dependence of the field level induced in BHM on the rf phase in the second tank

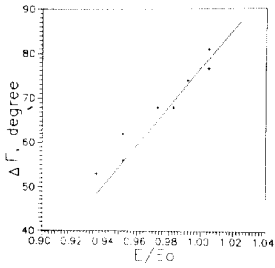


Fig. 5. The second tank rf bucket width at the half-height level depending on rf amplitude
— calculated
* experimental

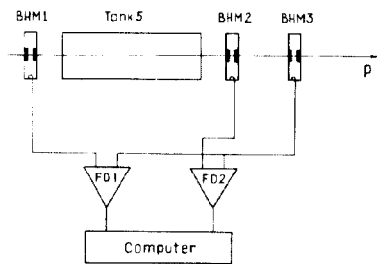


Fig. 6. The layout of time of flight measurement

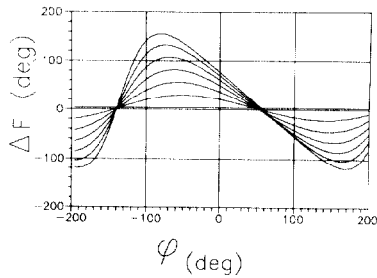


Fig. 7. The particles time of flight variation as functions of the rf phase in the fifth tank. The $\Delta\Phi$ value corresponds to the phase shift between the second and the third BHM

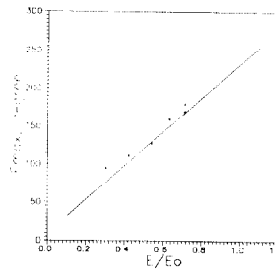


Fig. 8. The phase shift of the signal, induced in BHMs between extremums as a function of the rf amplitude in the fifth tank.
— calculated
* experimental

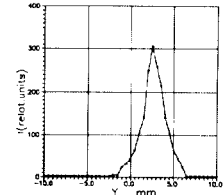
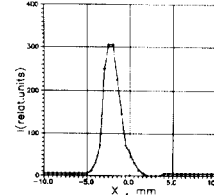


Fig. 9. Beam profiles at the energy of 100 MeV

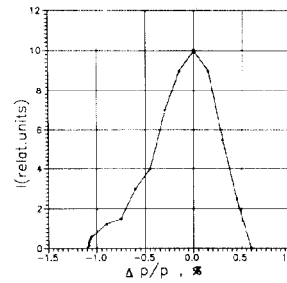


Fig. 10. Momentum spectrum of the 100 MeV beam

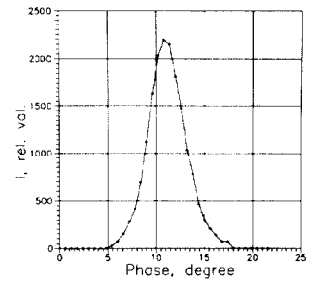


Fig. 11. Phase spectrum of the 100 MeV beam

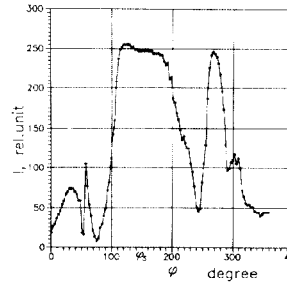


Fig. 12. Phase scan by using BHM

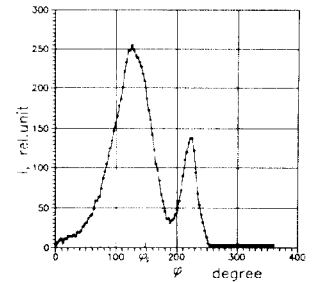


Fig. 13. Phase scan by using magnet bending